MOLECULAR AND CELLULAR BIOLOGY, Feb. 1997, p. 667–676 Vol. 17, No. 2
0270-7306/97/$04.00+0

Characterization of Reaper- and FADD-Induced Apoptosis in a Lepidopteran Cell Line

DOMAGOJ VUCIC,[1] SOMASEKAR SESHAGIRI,[2] AND LOIS K. MILLER[1,2]*

Department of Genetics[1] and Department of Entomology,[2]
The University of Georgia, Athens, Georgia 30602

Received 15 July 1996/Returned for modification 1 October 1996/Accepted 6 November 1996

Expression of the *reaper* gene (*rpr*) correlates with the initiation of apoptosis in *Drosophila melanogaster*. Transient expression of *rpr* in the lepidopteran SF-21 cell line induced apoptosis displaying nuclear condensation and fragmentation, oligonucleosomal ladder formation, cell surface blebbing, and apoptotic body formation. Inhibitors of ICE-family proteases *p35* and *crmA*, as well as members of the *iap* class of genes, Op-*iap* and D-*iap2*, but not *bcl-2* family members, blocked *rpr*-induced apoptosis. Mutational analysis of *rpr* provided no support for the proposed sequence similarity of Reaper and death domain proteins. Mutations in the N-terminal region of Reaper, which displays sequence similarity to Hid and Grim, other *Drosophila* gene products correlated with the initiation of apoptosis, suggested that these residues might be functionally important. The mammalian cDNA encoding FADD (Fas-associating protein with a death domain) also induced cell death in SF-21 cells, but death progressed more slowly and with features which distinguished it from *rpr*-induced apoptosis. Several *bcl-2* family members delayed or blocked FADD-induced cellular death. Thus, apoptosis initiated by Reaper progressed by a faster path which appeared to differ from that of FADD-induced apoptosis.

Apoptosis is a genetically regulated mechanism by which cells die in a characteristic morphological and biochemical pattern that includes the condensation and fragmentation of the nucleus, degradation of the chromosomal DNA into oligonucleosomal fragments, and blebbing of the plasma membrane, culminating in fragmentation of the cell into membrane-bound apoptotic bodies (34, 65). Many of the basic genetic, biochemical, and morphological features of apoptosis are conserved across animal phyla (9, 17, 27, 53, 60, 66, 67). Several classes of genes which regulate apoptosis are known to have counterparts in both invertebrates and vertebrates and probably represent central components of the apoptotic pathway. Other apoptotic regulatory genes may be less central and/or less conserved.

Three *Drosophila melanogaster* genes, *reaper* (*rpr*), *head involution defective* (*hid*), and *grim*, were recently identified within the chromosomal 75C1,2 region as inducers of apoptosis in cells selected to die during embryogenesis (11, 25, 64). In *Drosophila*, ectopic expression of *rpr*, which encodes a 65-amino-acid peptide (Reaper), induces death in cells in which it is expressed (26, 64) while induction of expression of an exogenous copy of *rpr* in a *Drosophila* cell line results in rapid death accompanied by membrane blebbing (44). Reaper-induced apoptosis is associated with an increase in ceramide levels (44) and involves activation of an ICE-family protease (63). *hid* and *grim* are predicted to encode a 415-amino-acid polypeptide (Hid) and 138-amino-acid polypeptide (Grim), respectively. Like *rpr*, ectopic expression of *hid* and *grim* in *Drosophila* induces cell death through activation of an ICE-family protease (25). Reaper, Hid, and Grim appear to act independently and share no extensive sequence homology, although a resemblance between the sequences of the N-terminal 14 amino acids of the three proteins was noted (11).

Based on a manual sequence alignment, Golstein and others proposed that Reaper may correspond to the death domains of the mammalian cytotoxic T-cell ligand effector Fas/APO-1L/CD95L and tumor necrosis factor receptor 1 (TNFR-1) (19, 24). When activated by binding of their respective ligands, TNFR-1 and Fas induce cell death which is dependent on a stretch of 80 to 90 amino acids in their cytoplasmic regions, termed the death domain (6, 42). Three cytoplasmic proteins, TRADD (32), FADD (7, 14), and RIP (51), also contain death domains, induce apoptosis upon overexpression, and associate with the death domains of TNFR-1 and/or Fas. The ability of TNFR-1, Fas, TRADD, and RIP to induce apoptosis resides in their death domains, but FADD-induced apoptosis involves a 117-amino-acid N-terminal region called the death effector domain (14). Deletion of 80 N-terminal amino acid residues of this domain of FADD results in a dominant negative mutant which abrogates Fas-induced apoptosis, ceramide generation, and activation of the ICE-family protease Yama/CPP32 (12) and also inhibits apoptosis induced by overexpression of TRADD and TNFR-1 (31). This suggests that FADD acts downstream of both the Fas and TNFR-1 death-stimulating signals. Through its death effector domain, FADD recruits FLICE/MACH, a polypeptide containing both a death effector domain and a region homologous to ICE-family proteases (5, 41), thus providing a physical link between receptors with death domains and the ICE-family proteases (23). Experimental evidence that *rpr* proceeds through a similar pathway remains to be established; ceramide generation and ICE-family protease activation are common to apoptotic pathways induced by a number of different induction signals.

The ICE-family proteases are cysteine-dependent, aspartate-specific proteases (caspases) which are implicated as phylogenetically conserved executioners of apoptosis based on their ability to induce apoptosis in nematodes, insects, and mammals (9, 40, 66) and by the ability of viral inhibitors of caspases to block apoptosis in a phylogenetically broad spectrum of animals. The product of the baculovirus gene *p35* is a stoichiometric inhibitor of the mammalian caspases ICE,

* Corresponding author. Phone: (706) 542-2294. Fax: (706) 542-2279. E-mail: miller@bscr.uga.edu.

ICH-1, ICH-2, and CPP32 and the nematode caspase CED-3 (9, 66). *p35* normally blocks apoptosis during baculovirus replication in insect cells (17) but can also block apoptosis caused by other signals and in diverse settings: in lepidopteran SF-21 cells, *p35* blocks apoptosis induced by actinomycin D (18) or ICE-family proteases (9); in *Drosophila*, *p35* blocks normal and X-ray-induced apoptosis (27) and also *rpr*- and *hid*-induced apoptosis (25, 26, 63); in *Caenorhabditis elegans*, *p35* can partially substitute for *ced-9* (53); and in mammalian cells, *p35* blocks apoptosis induced by serum withdrawal (46), nerve growth factor deprivation (38), or Fas and TNFR-1 (2). The cowpox virus *crmA* gene encodes a serpin-like protein which can block some, but not all, caspases (35, 57) and also blocks an aspartate-specific serine protease, granzyme B (45). CrmA inhibits apoptosis induced by TNFR-1, Fas, FADD, TRADD, and/or FLICE in some mammalian cells (14, 32, 41, 56).

The founder members of another class of apoptotic inhibiting genes, the inhibitor of apoptosis genes (*iap* genes), were identified by their ability to substitute for the baculovirus *p35* gene (3, 20) but are now known to represent a large family of apoptotic inhibitors found in insects and vertebrates (21, 26, 37, 49, 58). In addition to their ability to complement *p35* during baculovirus infection, the baculovirus Cp-*iap* and Op-*iap* genes block actinomycin D-induced apoptosis in SF-21 cells (18). Cp-*iap* can partially block *rpr*-dependent apoptosis in *Drosophila* developing eyes (26), while Op-*iap* partially blocks pro-ICE- and FADD-induced apoptosis in HeLa cells (21, 58). Members of the *iap* family have two or three tandem BIR (baculovirus *iap* repeat) motifs located at the amino terminus and the center of the protein. Most, but not all, *iap* gene products have a carboxy-terminal RING finger. The BIR motifs have a complex sequence with characteristic conserved residues (16), while the RING finger probably forms a cross-braced zinc-binding domain which is thought to participate in protein-protein interactions (8).

Bcl-2 is the founder member of a functionally diverse family of cell death regulators. Originally described for its role in B-cell lymphoma, *bcl-2* overexpression inhibits cell death induced by a variety of apoptotic stimuli in mammalian cell lines (48), partially substitutes for a related gene in nematodes, *ced-9* (28, 29, 60), and extends the survival of baculovirus-infected insect cells (1). Transcripts of a *bcl-2* homology, *bcl-x*, are alternatively spliced to produce an inhibitor of apoptosis, Bcl-x_L, and an apoptotic inducer, Bcl-x_S (4). The ability of *bcl-2* or *bcl-*x_L to block cell death induced by Fas or TNFR-1 appears to be dependent on the cell type, strength of death stimulus, and expression level of the anti-apoptotic genes (13, 33, 36, 39, 50, 52, 59). BAG-1, a Bcl-2 binding protein, enhances the antiapoptotic potential of Bcl-2 (54). The adenovirus E1B19K protein, a viral member of the Bcl-2 family (15), blocks apoptosis during adenovirus infection and transformation and also blocks tumor necrosis factor alpha- and anti-Fas antibody-induced apoptosis (62).

In this study, we demonstrate that *rpr* and FADD induce apoptosis in SF-21 cells and compare the nature of their apoptotic pathway(s) by determining whether members of the different classes of antiapoptotic genes can block *rpr*- and FADD-induced apoptosis. The SF-21 cell line is "preprimed" for apoptosis, undergoing a full apoptotic response to actinomycin D induction without additional protein or RNA synthesis (18). We also address the possible functional significance of previous sequence alignments of Reaper with Hid and Grim or mammalian death domain proteins by mutational analysis of Reaper. Our analyses suggest that *rpr*- and FADD-induced apoptosis proceeds by distinguishable pathways in SF-21 cells and that the previous sequence alignments of Reaper with death domain proteins are probably not significant.

MATERIALS AND METHODS

Cell line. *Spodoptera frugiperda* (Lepidoptera: Noctuidae) IPLB-SF-21 (SF-21) cells were maintained in TC-100 medium (Gibco BRL, Gaithersburg, Md.) supplemented with 10% fetal bovine serum (Intergen, Purchase, N.Y.) and 0.26% tryptose broth as previously described (43).

Plasmid construction and site-specific mutagenesis. All the plasmids used are pHSP70PLVI$^+$CAT based (18). The *cat* gene was removed from pHSP70PLVI$^+$CAT and replaced by the following fragments: in pHSP70PLVI$^+$Rpr, a *Bam*HI-*Eco*RV fragment from prpr40ka, containing the entire *rpr* cDNA (64); in pHSP70CrmAVI$^+$, an *Eco*RI-*Hin*dIII fragment from pGEMcrmA (47); in pHSP70Bcl-xVI$^+$, a *Cla*I-*Not*I fragment from pBSBcl-x (4); in pHSP70Bag-1 VI$^+$, a *Xho*I-*Not*I fragment from pSKIIBag-1 (54); in pHSDIAP2VI$^+$, an *Eco*RI fragment from pBSDIAP2 (26); in phspced9VI$^+$, a *Hin*dIII-*Spe*I fragment from pBS-SK(−)ced-9 (29); and in pHSP70PLVI$^+$FADD, a *Kpn*I-*Xho*I fragment from pcDNA3/FADD (14). Construction of pHSOp-IAPVI$^+$, pHSp35VI$^+$, pHSAd19KVI$^+$, pHSBcl-2VI$^+$ and pHSP70PLVI$^+$CAT was previously described (18). The sequence encoding the 65-amino-acid *rpr* open reading frame (ORF) was amplified by PCR with Pfu polymerase (Stratagene, La Jolla, Calif.) and the primers CRPR (ATATCCCGGGTAGTTACTCGAATCCTCA TTGCG) plus NRPR (GAAGATCTACAATGGCAGTGGCATTCTAC). Sequences encoding the first 37 and last 36 amino acids of the 65-amino-acid *rpr*-ORF were amplified by PCR with Pfu polymerase (Stratagene) and the primers NRPR plus MCRPR (ATATCCCGGGTTAGGTGGCCAGGAATCT CCA) and CRPR plus MNRPR (GAAGATCTACAATGCTGGCCACCGTCG TCCTG), respectively. The resulting products were digested with *Bgl*II and *Xma*I and subcloned into the *Bgl*II and *Pst*I sites of pHSP70PLVI$^+$CAT to generate pHSP70PLVI$^+$RPR-ORF, pHSP70PLVI$^+$RPR(1–37), and pHSP70PLVI$^+$RPR (29–65), respectively. pHSP70PLVI$^+$RPR-ORF was digested with *Bsm*I, and the overhanging ends were removed with T4 DNA polymerase to generate pHSP70 PLVI$^+$RPR-ORF/fs with the frameshift in the 65-amino-acid *rpr* ORF after the fourth amino acid. pHSP70PLVI$^+$Epi-RPR was constructed to fuse an HA epitope tag (YPYDVPDYA) onto the N terminus of the *rpr* 65-amino-acid ORF. Site-specific mutagenesis was performed on pHSP70PLVI$^+$RPR-ORF with the Transformer site-directed mutagenesis kit (Clontech, Palo Alto, Calif.) selection primer KPNRPRNHE (CAGCAGAGTCGCTAGCGATGTAAACGATGG) and the mutagenic primers FRPRA5 (CAATGGCAGTGGCAGCCTACATA CCCGATC), YARPR6 (GCAGTGGCATTCGCGATACCCGATCAG), ARPRN11 (CATACCCGATCAGAACACTCTGTTGCGG), EARPR29 (CTC CGCTTGCGCGCGTCACAG TGGAC), LRPTA35 (CAGTGGAGATTCGC GGCCACCGTCGTC), CARPR49 (CCAGTACACTTCTGCGCATCCGAAG ACCG), and PARPR8 (GTGGCATTCTACATAGCCGACCAGGCGACTC TG) to generate a series of single and double mutants.

DAPI staining. SF-21 cells (5×10^5 per 35-mm tissue culture dish) were transfected with 6 μg of indicated plasmids by Lipofectin-mediated transfection (Gibco BRL). The cells were heat shocked 20 h posttransfection for 30 min at 42°C. At 10 h after the heat shock, the cells were washed once with phosphate-buffered saline (PBS; pH 6.2), fixed with a mixture of methanol and acetone (1:1) for 10 min, washed once with PBS, stained with 1 μg of 4′,6′-diamidino-2-phenylindole (DAPI; Sigma, St. Louis, Mo.) per ml for 10 min, washed once with PBS, and observed under UV light.

DNA fragmentation and viability assays. SF-21 cells were transfected and heat shocked as described for DAPI staining. DNA fragmentation and viability assays were described previously (17, 18).

Immunoblots. SF-21 cells were transfected with appropriate plasmids and heat shocked as described above. The cells were harvested 1 to 10 h after the heat shocking and lysed in sodium dodecyl sulfate SDS sample buffer (43). Total protein samples were separated by sodium dodecyl sulfate-polyacrylamide gel electrophoresis (15% polyacrylamide) and transferred to Immobilon-P membranes (Millipore, Bedford, Mass.) by electrophoresis for 16 h at 30 V. The membranes were blocked for 1 h at room temperature with 1× TBST (0.05% Tween 20) containing 5% dry milk and then immunoblotted for 2 h with polyclonal anti-Reaper antiserum, diluted 1:1,000 (obtained from G. J. Pronk, Chiron Corp.); monoclonal 4D7 antibody directed against human Bcl-2 protein, diluted 1:5,000 (Pharmingen, San Diego, Calif.); or polyclonal antibody directed against human Bcl-x_L protein, diluted 1:5,000 (Transduction Laboratories, Lexington, Ky.). Anti-rabbit immunoglobulin G-horseradish peroxidase conjugate (Amersham, Little Chalfont, England), diluted 1:16,000, or peroxidase-labelled anti-mouse antibody, diluted 1:16,000, was used as the secondary antibody, and the blots were developed by the enhanced chemiluminescence system (Amersham).

Multiple-sequence alignment. The sequence alignment of Reaper and death domain proteins was performed with the PileUp program of the Genetics Computer Group program package with a gap penalty of 2.1 and a gap extension penalty of 0.2. The shading assignment was accomplished with the Boxshade program (generated by Kay Hofmann).

GenBank/EMBL accession numbers for the sequences used were L36529 for human P84, U25994 for mouse RIP, L41690 for human TRADD, M28880 for human ankyrin, U21731 for *C. elegans unc44*, X84709 for human FADD, M67454 for human Fas, M63121 for mouse TNFR-1, X51397 for mouse MyD88, L08476

for *Drosophila pelle*, X76104 for human DAP-kinase, S47168 for *C. elegans unc5*, M14764 for human NGFR, M59501 for *Drosophila tube*, and L31631 for *Drosophila reaper.*

RESULTS

Reaper induces apoptosis in SF-21 cells. To determine whether the *Drosophila* gene *rpr* can induce apoptosis in SF-21 cells, we transiently expressed *rpr* by transfecting the cells with pHSP70PLVI$^+$Reaper, a plasmid containing the entire *rpr* cDNA under the control of the *Drosophila* hsp70 promoter, and heat shocking them 20 h posttransfection. At 2 to 3 h after induction of *rpr* expression by heat shocking, cells began to exhibit membrane blebbing. By 8 to 10 h after the heat shock treatment, cells transfected with *rpr* showed extensive membrane blebbing and apoptotic body formation (Fig. 1D); blebbing was not observed in control cells transfected with pHSP70PLVI$^+$CAT (Fig. 1B). To determine if *rpr*-induced membrane blebbing of SF-21 cells is accompanied by nuclear condensation, we stained cells with the fluorescent DNA stain, DAPI. Nuclear condensation and fragmentation were apparent in cells exhibiting membrane blebbing following cotransfection with *rpr* (Fig. 1C) and absent in cells transfected with *cat* alone (Fig. 1A). Therefore, *rpr* induces cell death in SF-21 cells with the characteristic morphological features of apoptosis, including nuclear condensation and fragmentation, membrane blebbing and apoptotic body formation.

We PCR amplified the sequence encoding only the 65-amino-acid *rpr* ORF and placed the *rpr* ORF under hsp70 promoter control to generate pHSP70PLVI$^+$Rpr-ORF. Transient expression of *rpr* ORF from pHSP70PLVI$^+$Rpr-ORF induced cell death to the same extent as pHSP70PLVI$^+$Rpr, containing the entire *rpr* cDNA as determined by the rapidity and extent of membrane blebbing, as well as by cell viability assays (see below); therefore, pHSP70PLVI$^+$Rpr-ORF was used in all subsequent experiments to provide *rpr.*

Inhibitors of ICE-family proteases and *iap* genes block *rpr*-induced apoptosis. To assess the nature of the apoptotic pathway induced by *rpr*, we determined whether several known antiapoptotic genes can block *rpr*-induced apoptosis in SF-21 cells. Cotransfection of *rpr* and *cat* induced apoptosis in 31 to 35% of the cells compared to that in cells transfected with the *cat* gene alone (Fig. 2A). Cotransfection of *rpr* with plasmids expressing the cowpox virus gene *crmA* or the baculovirus gene *p35*, which encode inhibitors of caspases, reduced the level of apoptosis three- and ninefold, respectively (Fig. 2A). This is consistent with previous studies that implicate the involvement of a caspase in *rpr*-induced apoptosis (26, 44, 63). We also tested two members of the *iap* class of antiapoptotic genes, the baculovirus Op-*iap* and *Drosophila* D-*iap2*, for their ability to block *rpr*-induced apoptosis in SF-21 cells. As shown in Fig. 2A, *rpr*-induced apoptosis was reduced ninefold by Op-*iap* and fourfold by D-*iap2*. *rpr*-induced nuclear condensation and membrane blebbing were also abolished when cells were cotransfected with plasmids expressing *rpr* cDNA and Op-*iap* (Fig. 1E and F).

bcl-2 family members (adenovirus E1B19K, *C. elegans ced-9*, human *bcl-2*, and human *bcl-x$_L$*) exhibited little or no ability to block *rpr*-induced apoptosis in SF-21 cells (Fig. 2A). We additionally tested the possibility that a Bcl-2 binding protein, BAG-1, is required for Bcl-2 to exert its antiapoptotic effect in SF-21 cells. However, cotransfection of plasmids expressing *bcl-2* and *bag-1* failed to protect SF-21 cells against *rpr*-induced apoptosis (Fig. 2A). To determine whether the inability of *bcl-2* or *bcl-x$_L$* to block *rpr*-induced apoptosis was due to the absence of Bcl-2 or Bcl-x$_L$ in the presence of Reaper, we examined the levels of Bcl-2 or Bcl-x$_L$ by Western blot analysis. In the presence or absence of Reaper, substantial levels of both Bcl-2 and Bcl-x$_L$ were observed 1.5 h after heat shock, and these levels persisted through 10 h after heat shock (Fig. 2B), the time at which the viability assays (Fig. 2A) were performed. Although a significant proportion of the cells were undergoing apoptosis in the presence of Reaper, the levels of Bcl-2 and Bcl-x$_L$ were remarkably similar to those observed for the *cat* controls in which apoptosis did not occur. Bcl-x$_L$ produced in SF-21 cells corresponded in size to Bcl-x$_L$ made in the mammalian Jurkat cell line (Fig. 2B, lane 11). Previous studies showed that Bcl-2 produced in SF-21 cells is similar in size to that produced in human AT3 cells (16) and is active in delaying SF-21 cell death during baculovirus infection (1). Furthermore, Bcl-2 and Bcl-x$_L$ were both able to block FADD-induced apoptosis in SF-21 cells up to 24 h after heat shock (see below); therefore, it is clear that both these gene products are synthesized in a functional form in SF-21 cells. Thus, although they are expressed and are present 10 h after the heat shock, *bcl-2* and *bcl-x$_L$* do not block *rpr*-induced apoptosis in SF-21 cells.

In control experiments (results not shown), we determined that the inhibitors which we tested, including Op-IAP, DIAP-2, P35, CrmA, Ced-9, Bag-1, Bcl-2, Bcl-xL, E1B19K, and a combination of Bag-1 and Bcl-2, did not induce apoptosis in the absence of *reaper.*

Mutational analysis of Reaper. Two visual amino acid sequence alignments have suggested that Reaper may belong to the group of proteins with death domains (Fig. 3A) (19, 24). According to these alignments, several amino acid residues of Reaper show identity or similarity to amino acid residues that are conserved in a short cytoplasmic region of cell surface receptors for tumor necrosis factor and Fas ligand, TNFR-1 and Fas, referred to as the death domain. Inspection of this alignment, however, reveals very few identical sequences; only one amino acid, a leucine at position 35 (L35) in the reaper sequence, is rigorously conserved (Fig. 3A). Computer searches for additional proteins containing homology to known death domains significantly enlarged the group of proteins with death domains to include several new mammalian, *Drosophila*, and *C. elegans* proteins (22, 30). However, none of the homology searches based on the death domain sequences of TNFR-1 and Fas suggested that Reaper belongs to this family. Figure 3C shows a computer-generated sequence alignment that includes all the former and newly assigned members of the death domain family as well as Reaper.

A second possible sequence relationship has been noted for the N-terminal residues of Reaper, Hid and Grim, *Drosophila* proteins which have been ascribed a function in inducing apoptosis during *Drosophila* development (11, 25). The proposed alignment of the N-terminal 14 amino acid residues of these three proteins is shown in Fig. 3B.

We investigated the effects of mutagenizing individual conserved amino acid residues of Reaper to assess the significance of these sequence alignments. The significance of the sequence similarity of the 11 N-terminal residues of Reaper and Hid was examined by mutating the conserved F5 or Y6 residue of Reaper to alanine (A) and then assessing the ability of plasmids containing these mutant *rpr* genes to induce apoptosis in SF-21 cells (Fig. 4A). Both the F5A and Y6A mutations resulted in a twofold reduction in the percentage of cells which underwent apoptosis in response to *rpr* transfection, indicating that these residues have a role in, but are not individually essential for, *rpr* proapoptotic activity. Mutation of residue P8 of Reaper, which is conserved in Reaper, Hid, and Grim (Fig. 3B), to alanine (A) did not affect the ability of Reaper to induce apoptosis in SF-21 cells (data not shown).

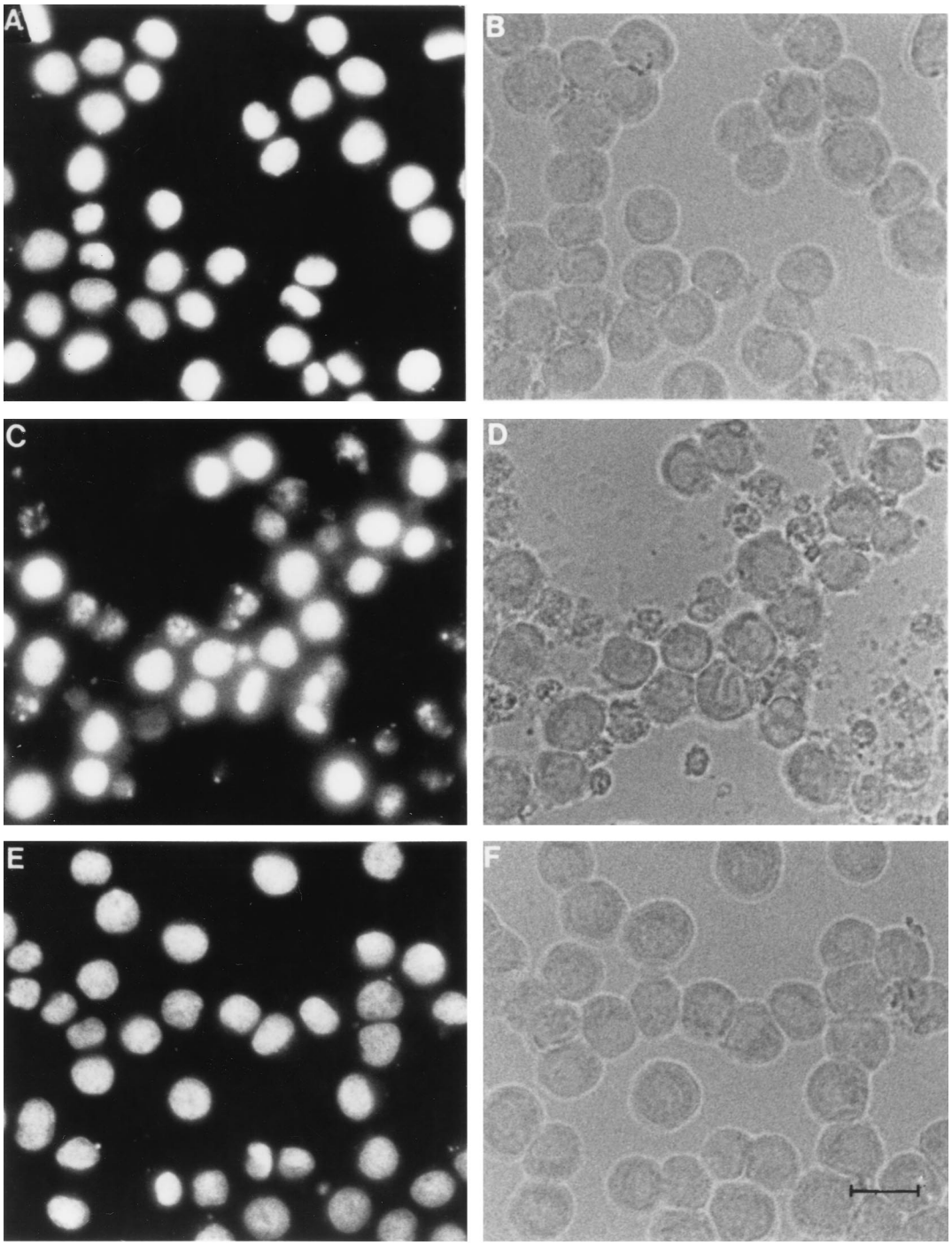

FIG. 1. Nuclear condensation and fragmentation are induced by *rpr* in SF-21 cells and can be blocked by Op-*iap*. SF-21 cells were transfected with plasmids expressing control *cat* gene (A and B), *rpr* and *cat* (C and D), or *rpr* and Op-*iap* (E and F) (the *cat*-expressing plasmid was cotransfected with *rpr* in panels C and D as a control for Op-*iap* cotransfection in panels E and F). Cells were stained with DAPI 10 h after induction of gene expression by heat shock. (A, C, and E) DAPI staining in cells viewed under UV light; (B, D, and F) the same field in phase-contrast microscopy. Bar, 25 μm.

Additional mutations were made to test the significance of previous alignments of Reaper with the death domains of TNFR-1 and Fas (19, 24). Residue A11 of Reaper was previously aligned (Fig. 3A) with residues in Fas and TNFR-1 which are known to be essential for their activity: V238 of Fas and L351 of TNFR-1. Mutations of V238 and L351 to asparagine (N) abolish the proapoptotic activity of these genes in cell culture (55), and, in the case of Fas, the V238N mutation is the basis for the lpr phenotype in mice (61). Mutation of the A11 residue of Reaper to asparagine (i.e., the A11N mutation) had no apparent effect on the apoptotic activity of *rpr* in SF-21 cells (Fig. 4A). The longest stretch of Reaper residues aligning with TNFR-1/Fas were amino acids L27, R28, and E29. These residues were considered "conserved" in the original alignments

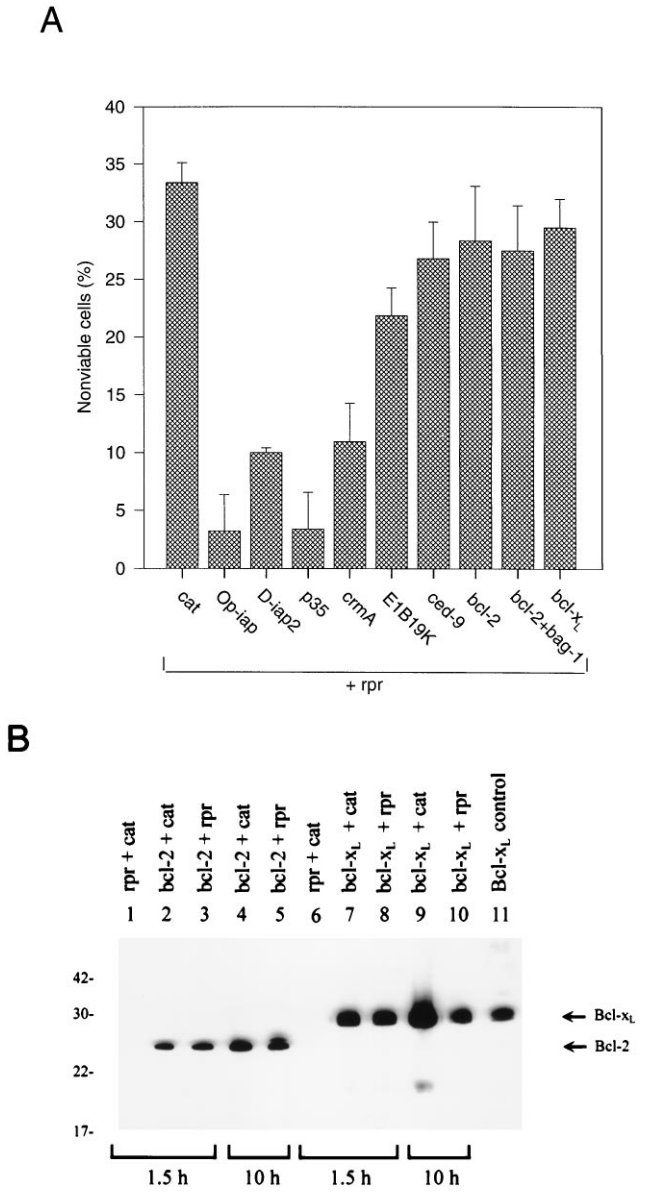

FIG. 2. (A) The ability of antiapoptotic genes to protect against *reaper*-induced apoptosis in SF-21 cells. Cells were cotransfected with plasmids expressing the *rpr* ORF plus *cat*, Op-*iap*, D-*iap2*, *p35*, *crmA*, E1B19K, *ced-9*, *bcl-2*, *bcl-2* plus *bag-1*, or *bcl-x$_L$*. Cell viability was determined by trypan blue exclusion 10 h after the heat shock. The results are relative to the viability of cells transfected with the *cat* gene alone (set at 100% viability) and represent at least four independent experiments for each cotransfected combination. Standard deviations are indicated by the error bars. (B) Immunoblot analysis of the expression of *bcl-2* and *bcl-x$_L$* in the viability assay described in the legend to panel A. SF-21 cells were cotransfected with *rpr* and *cat* (lane 1 and 6), *cat* and *bcl-2* (lanes 2 and 4), *rpr* and *bcl-2* (lanes 3 and 5), *cat* and *bcl-x$_L$* (lanes 7 and 9), and *rpr* and *bcl-x$_L$* (lanes 8 and 10). Cells were harvested 1.5 h (lanes 1 to 3 and 6 to 8) and 10 h (lanes 4, 5, 9, and 10) after the heat shock. Equal amounts of cell lysates were analyzed by SDS-polyacrylamide gel electrophoresis followed by Western blotting with anti-Bcl-2 monoclonal antibody (lanes 1 to 5) or anti-Bcl-x$_L$ polyclonal antibody (lanes 6 to 11). Lane 11 contains lysate from Jurkat cells overexpressing human Bcl-x$_L$ for comparison. Molecular mass markers (in kilodaltons) are shown on the left.

(Fig. 3A), but only E29 exhibits some "identity" with death domain family members in computer-generated alignments (e.g., Fig. 3C). Mutation of E29 to alanine (E29A) had no observable effect on the ability of *rpr* to induce apoptosis in the SF-21 cell viability assay (Fig. 4A). The E29A mutation did not affect the proapoptotic activity of *rpr* in *Drosophila* SL2 cells either (10). Similarly, L35, a residue rigorously conserved in the original alignments and relatively conserved in the current alignment, was mutated to alanine (L35A) with no observable effect on *rpr* apoptotic activity (Fig. 4A). Three double mutants were also constructed and tested for apoptotic activity to determine if combinations of these "conserved" residues might have additive or synergistic effects. Combinations of F5A and L35A mutations, A11N and L35A mutations, and E29A and A11N mutations had no observable additive or synergistic effects (Fig. 4A).

Several additional *rpr* mutants were tested. Mutation of the sole cysteine of *rpr* to alanine, C49A, resulted in a slight reduction in *rpr* apoptotic activity (Fig. 4A) which may be correlated with reduced levels of mutant protein observed in transfected cells shortly after heat shock induction (Fig. 4B). The mild reduction, if any, observed for this mutant indicates that it is not essential for *rpr* apoptotic activity, suggesting that neither disulfide bonding nor oxidation of this sulfhydryl group is involved in *rpr* activity.

We constructed two truncated forms of *rpr* ORF, one encoding the first 37 amino acids [*rpr*(1–37)], and the other encoding the last 36 amino acids [*rpr*(29–65)] of the Reaper protein, and a frameshift mutant, *rpr*-fs, which was frameshifted after the fourth amino acid of Reaper. Transient expression of *rpr*(1–37), *rpr*(29–65), or *rpr*-fs did not induce apoptosis; the last mutant served as negative control (Fig. 4A). An additional construct, Epi-*rpr*, contained a N-terminally located sequence encoding the HA epitope tag and failed to induce apoptosis (Fig. 4A). In addition, we examined if the *rpr* truncations, *rpr*-fs and Epi-*rpr*, caused a dominant-negative phenotype, but none of them significantly reduced the levels of *rpr* ORF-induced apoptosis when cotransfected individually with *rpr* ORF (data not shown).

To assess the levels of Reaper produced by each of these plasmids, we performed immunoblot analysis of transfected cell extracts with a polyclonal Reaper-specific antibody. A significant level of expression from *rpr* ORF was observed 80 min after heat shocking, and a similar level of expression was also evident for the mutants with approximately 50% of the activity of *rpr* ORF (F5A, Y6A, and F5A/L35A) (Fig. 4B, lanes 1 to 3 and 8). Mutants with other point mutations showed comparable levels of expression (lanes 4 to 6, 9, and 10), with the exception of expression of the C49A mutant (lane 7), which was reduced. The two inactive *rpr* truncations, *rpr*(1–37) and *rpr*(29–65), as well as *rpr*-fs, did not express detectable levels of protein product (lanes 11 to 13). This was expected for *rpr*-fs and *rpr*(1–37), but not for *rpr*(29–65), as Reaper-specific antibody was raised against the C-terminal 15 amino acids of Reaper (44). A high level of expression of Epi-*rpr* was detected, although it showed no apoptotic activity (lane 14). Thus, the N-terminal HA epitope tag in Epi-*rpr* disrupts its ability to induce apoptosis.

FADD- and *rpr*-induced cell death in SF-21 cells have distinct features. We also determined whether expression of the death domain protein FADD could induce cell death in SF-21 cells and, if so, the nature of the cell death pathway activated by this protein. For this purpose, FADD was placed under the control of the *Drosophila* hsp70 promoter. Transient expression of FADD induced cell death in SF-21 cells but much more slowly than *rpr*. Whereas *rpr* induced extensive cell blebbing by 6 h after heat shock (Fig. 5B), FADD-transfected cells (Fig. 5C) appeared indistinguishable from control *cat*-transfected SF-21 cells (Fig. 5A) at that time. FADD-transfected cells displayed apoptotic morphological alterations such as ruffling

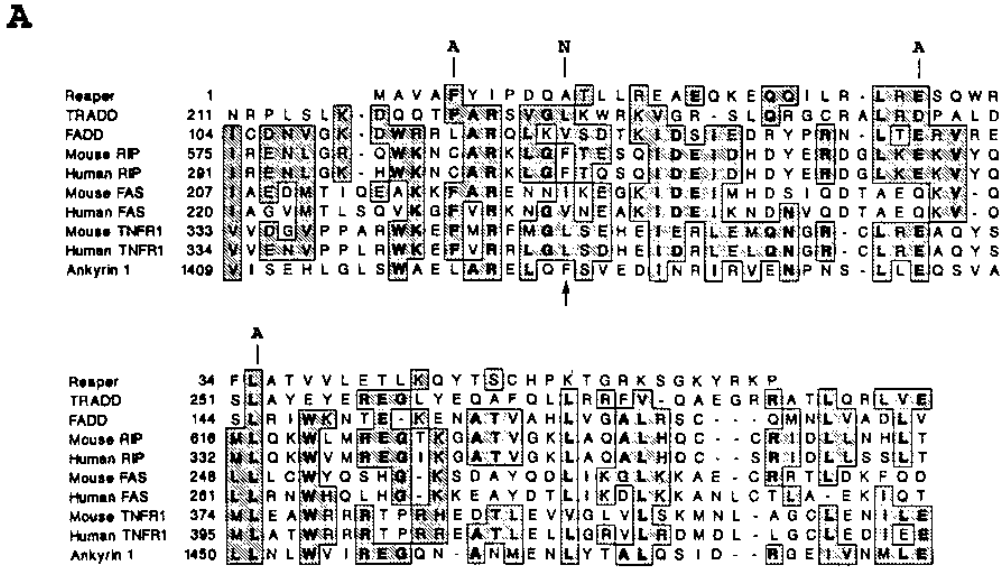
A
Reaper
TRADD
FADD
Mouse RIP
Human RIP
Mouse FAS
Human FAS
Mouse TNFR1
Human TNFR1
Ankyrin 1

A
Reaper
TRADD
FADD
Mouse RIP
Human RIP
Mouse FAS
Human FAS
Mouse TNFR1
Human TNFR1
Ankyrin 1

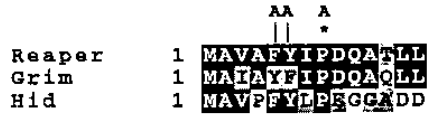
B
AA A
*
Reaper 1 MAVAFYIPDQATLL
Grim 1 MAIAYFIPDQAQLL
Hid 1 MAVPFYLPEGGAADD

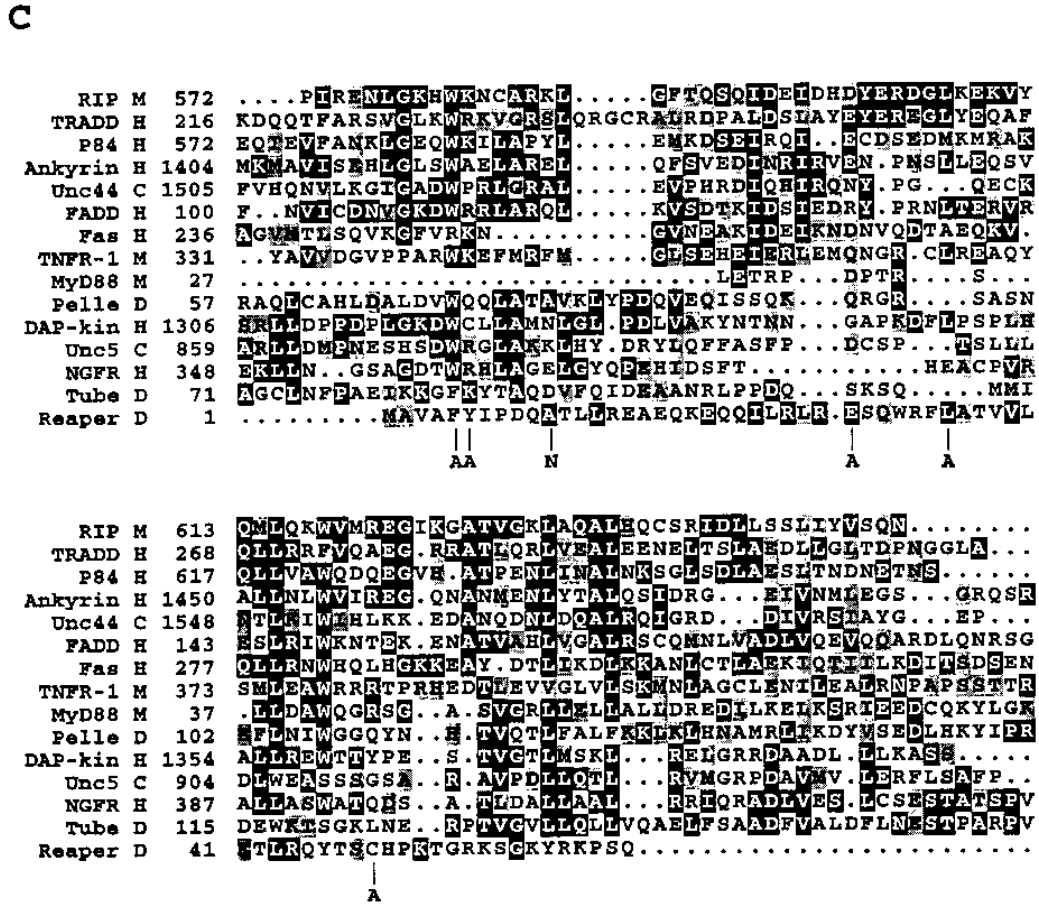
C
RIP M 572
TRADD H 216
P84 H 572
Ankyrin H 1404
Unc44 C 1505
FADD H 100
Fas H 236
TNFR-1 M 331
MyD88 M 27
Pelle D 57
DAP-kin H 1306
Unc5 C 859
NGFR H 348
Tube D 71
Reaper D 1
AA
N
A
A
RIP M 613
TRADD H 268
P84 H 617
Ankyrin H 1450
Unc44 C 1548
FADD H 143
Fas H 277
TNFR-1 M 373
MyD88 M 37
Pelle D 102
DAP-kin H 1354
Unc5 C 904
NGFR H 387
Tube D 115
Reaper D 41
A

FIG. 3. (A) Previously proposed alignments of Reaper with death domains (19). Amino acid changes made in mutational analysis of Reaper are indicated by the letters above the sequence alignment. (B) Previously proposed alignments of the first 14 amino acids of Reaper, Grim, and Hid (11, 25). Amino acid changes made in mutational analysis of Reaper are indicated by the letters above the sequence alignment. The asterisk denotes an amino acid change in an absolutely conserved residue. (C) Amino acid sequence alignment of Reaper with various death domains aligned with computer assistance. Amino acids identical to the most common amino acid are shown in black boxes, and similar amino acids are shown in shaded boxes. Letters to the right of the protein names designate the organism of gene origin (H, human; M, mouse; D, *Drosophila*; C, *C. elegans*), and numbers represent the positions of amino acids in the relevant protein. Amino acid changes made in the mutational analysis of Reaper are indicated by the letters below the sequence alignment.

of the membranes and detachment from the plates 24 h after heat shocking (Fig. 5D), but apoptosis accompanied by extensive membrane blebbing and apoptotic body formation was not evident until 48 h after heat shocking (Fig. 5E). This visually observed temporal difference in the induction of apoptosis by *rpr* and FADD was supported by oligonucleosomal ladder formation (Fig. 6). Formation of oligonucleosomal ladders was evident 48 h after heat shocking, when SF-21 cells were cotransfected with FADD and *cat* (Fig. 6, lane 8), but not at 10 h or 24 h after heat shocking (lanes 6 and 7). In contrast, SF-21 cells cotransfected with *rpr* and *cat* exhibited oligonucleosomal ladder formation as early as 10 h after the heat shock (lane 2). Cells transfected with *cat* alone showed no DNA ladder formation at 10 h or 48 h after transfection (lanes 1 and 12).

To assess the ability of FADD to cause cell death and to determine the nature of its apoptotic pathway in SF-21 cells, we cotransfected SF-21 cells with FADD and a control *cat*-expressing plasmid or plasmids expressing antiapoptotic genes and examined cell viability at 24 h after induction by heat shock. Cotransfection of FADD with *cat* resulted in a cytopathic effect in 34% of the cells (Fig. 7). Cotransfection of FADD with Op-*iap*, *p35*, *crmA*, and E1B19K reduced the percentage of cells exhibiting a FADD-induced cytopathic effect approximately twofold (Fig. 7). Among the *bcl-2* family members, *ced-9* had limited or no ability to block the FADD-induced cytopathic effect, but mammalian *bcl-2* (alone or with *bag-1*) and, to a greater extent, *bcl-x*$_L$, efficiently inhibited the FADD-induced cytopathic effect (Fig. 7). Op-*iap* and *p35* blocked oligonucleosomal ladder formation induced by either *rpr* or FADD (Fig. 6, lanes 3, 4, 9, and 10). In contrast, *bcl-x*$_L$ was able to inhibit the formation of the oligonucleosomal ladder induced by FADD but not by *rpr* (lanes 5 and 11). Thus, FADD induced cellular death in SF-21 cells with characteristic apoptotic features, although with a significant temporal delay when compared to *rpr*. Furthermore, several *bcl-2* family members efficiently inhibited FADD-induced cellular death, while the caspase inhibitors and Op-*iap* reduced the level of FADD-induced cellular death approximately twofold.

DISCUSSION

In this study, we have analyzed the nature of the apoptotic response induced by the *Drosophila* gene *reaper*. The role of Reaper in regulating apoptosis has been demonstrated in *Drosophila* embryos (64) and developing eyes (26, 63) and in a *Drosophila* cell line (44). Here, we have established that Reaper can induce cellular death in a lepidopteran cell line, SF-21, with all the morphological and biochemical characteristics of apoptosis as demonstrated by nuclear condensation and fragmentation, membrane blebbing and apoptotic body formation, and formation of an oligonucleosomal DNA ladder (Fig. 1, 5, and 6).

Reaper-induced apoptosis in SF-21 cells can be blocked by two classes of antiapoptotic genes. The first class consists of genes that encode inhibitors of caspases, *p35* and *crmA*. The baculovirus *p35* gene was previously reported to block *rpr*-induced apoptosis in *Drosophila* developing eyes (26, 63) and to block apoptosis induced by viral infection (17), actinomycin D (18), and p32 ICE (9) in SF-21 cells. We have shown that *p35* is very effective in blocking *rpr*-induced apoptosis in SF-21 cells. The cowpox virus gene *crmA* also blocked *rpr*-induced apoptosis in SF-21 cells, although not as efficiently as *p35* did (Fig. 2A). One explanation of this result is that *crmA* may not interact as efficiently as *p35* with one or more of the insect proteases involved. These results indicate that *rpr*-induced apoptosis in SF-21 cells proceeds through a pathway involving the activation of a caspase.

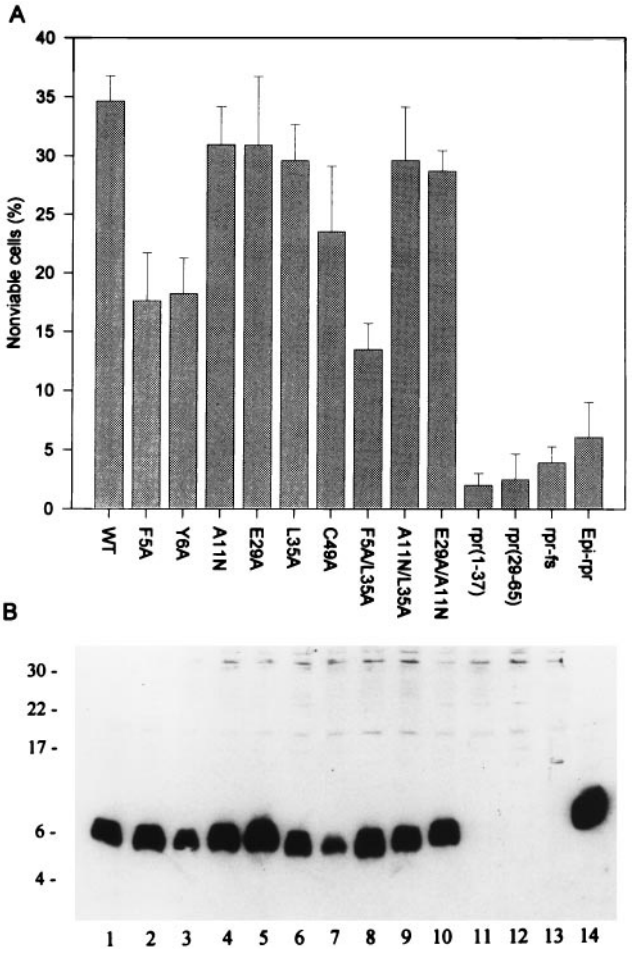

FIG. 4. Apoptotic activities of *reaper* mutants. SF-21 cells were transfected with *rpr* ORF (WT), or the following *rpr*-ORF mutants: *rpr*F5A, *rpr*Y6A, *rpr*A11N, *rpr*E29A, *rpr*L35A, *rpr*C49A, *rpr*F5A/L35A, *rpr*A11N/L35A, *rpr*E29A/A11N, truncated forms of *rpr* [*rpr*(1–37) and *rpr*(29–65)], *rpr*-fs, and Epi-*rpr*. Cell viability was determined as in Fig. 2A. The results shown represent the mean values of at least three independent experiments. Standard deviations are indicated by the error bars. (B) Immunoblot analysis of the expression of the *rpr* clones described in panel A. Transfected SF-21 cells were harvested 80 min after the heat shock. Equal amounts of cell lysates were analyzed by SDS-polyacrylamide gel electrophoresis followed by Western blotting with anti-Reaper antiserum. Molecular mass markers (in kilodaltons) are shown on the left.

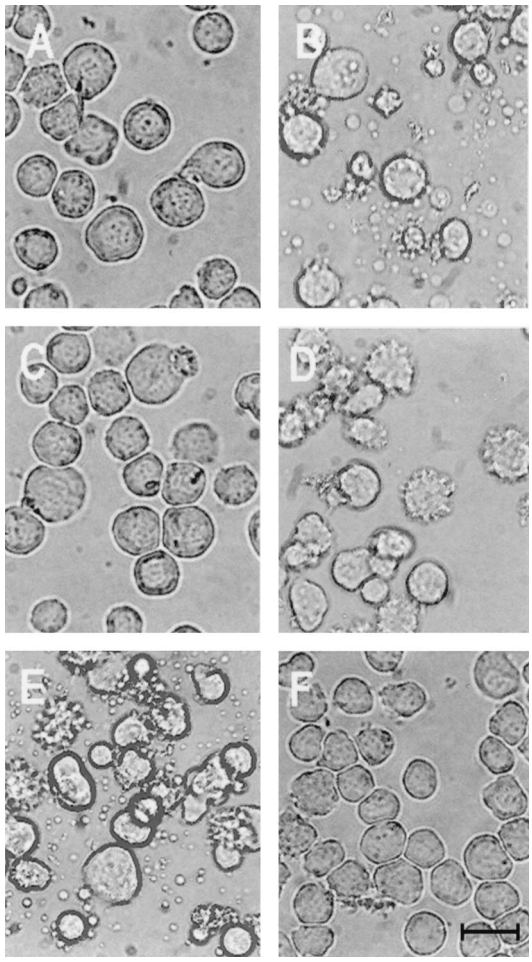

FIG. 5. FADD-induced cell death in SF-21 cells is delayed relative to *rpr*. SF-21 cells were transfected with *cat* (A and F), *rpr* (B), or FADD (C to E). Phase-contrast micrographs were taken 6 h (A to C), 24 h (D), or 48 h (E and F) after the heat shock. Bar, 25 μm.

The other class of genes that can block *rpr*-induced apoptosis in SF-21 cells consists of *iap* genes. Hay et al. (26) have shown that *Drosophila iaps* (D-*iap1* and D-*iap2*) block apoptosis induced by *rpr* in *Drosophila* developing eyes and that baculovirus Cp-*iap* is less effective in its *rpr*-inhibiting activity than are *Drosophila iap* genes. We have demonstrated that baculovirus Op-*iap* is a potent inhibitor of all manifestations of *rpr*-induced cell death in SF-21 cells (Fig. 1, 2, and 6) and that *Drosophila* D-*iap2* blocks *rpr*-induced apoptosis in SF-21 cells but not as well as Op-*iap* does (Fig. 2A). These differences may reflect organism specificity; the hosts of the baculoviruses from which Cp-*iap* and Op-*iap* are derived belong to a different order than *Drosophila.*

A third class of antiapoptotic genes, the *bcl-2* family members (*bcl-2*, *bcl-x_L*, *ced-9*, E1B19K, and *bcl-2*, together with *bag-1*), did not effectively block *rpr*-induced apoptosis in SF-21 cells (Fig. 2A). Clem and Miller (18) have previously demonstrated that despite high levels of expression of *bcl-2* and adenovirus E1B19K, neither of the products of these genes exhibited any observable antiapoptotic activity in SF-21 cells when apoptosis was induced by *p35* mutant *Autographa californica* nuclear polyhedrosis virus (Ac*M*NPV) or actinomycin D. We have examined the levels of expression of both *bcl-2* and *bcl-x_L* and determined that lack of expression is unlikely to be the cause of their failure to block *rpr*-induced apoptosis. Furthermore, we and others (1) have shown the that Bcl-2 and Bcl-x_L are functional in delaying or inhibiting cell death induced by some signals when expressed in SF-21 cells or their clonal derivative, SF-9 cells. Thus, *rpr* induces cellular death in SF-21 cells through a pathway in which *bcl-2* family members do not play an active role or are unable to counteract the induction signal effectively or act upstream of *rpr.*

Our mutational analysis of Reaper has addressed several issues concerning its relatedness to other apoptosis-inducing proteins. We have found that mutations of two amino acid residues at the N terminus of Reaper decrease its apoptotic activity and that addition of an N-terminal tag disrupts its function. These two N-terminal residues correspond to residues at equivalent positions of Hid, suggesting that the sequence similarity of these two proteins in this region may be significant to their apoptosis-inducing functions. However, an alanine substitution for residue P8 of Reaper, which is found at the equivalent position in Hid and Grim, did not alter the ability of Reaper to induce apoptosis. Taken together with mutational analysis by Chen et al., which showed that eliminating 14 amino acids from the N terminus of Reaper reduced the proapototic activity of Reaper by only 50% (10), our result suggests that the functional significance of this short homologous region remains ambiguous.

Mutational analysis of residues originally proposed to be conserved between Reaper and death domain proteins (19, 24) failed to support a functional significance for these proposed sequence alignments. Mutations in the residues that showed the strongest conservation displayed no observable alteration

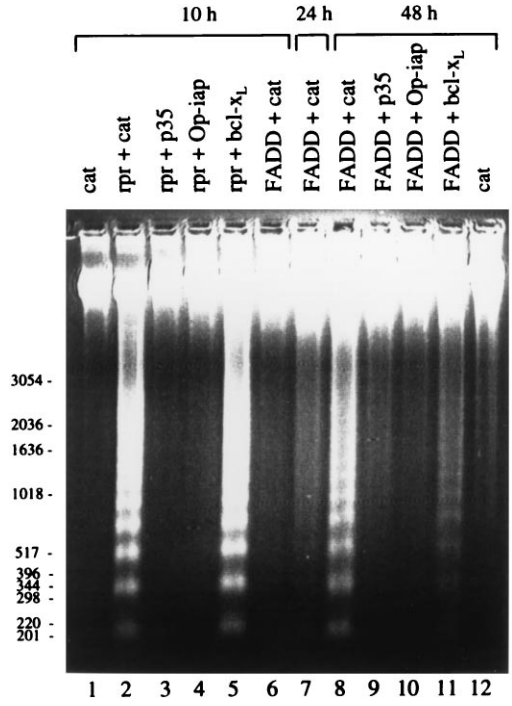

FIG. 6. *rpr* and FADD induce nucleolytic degradation of chromatin into oligonucleosomal ladder-sized fragments of DNA. SF-21 cells were transfected with the control *cat* gene (lanes 1 and 12), *rpr* and *cat* (lane 2), *rpr* and *p35* (lane 3), *rpr* and Op-*iap* (lane 4), *rpr* and *bcl-x_L* (lane 5), FADD and *cat* (lanes 6 to 8), FADD and *p35* (lane 9), FADD and Op-*iap* (lane 10), or FADD and *bcl-x_L* (lane 11). Total DNA was harvested 10 h (lanes 1 to 6), 24 h (lane 7), or 48 h (lanes 8 to 12) after heat shock and analyzed by agarose gel electrophoresis. Size markers (in base pairs) are indicated on the left.

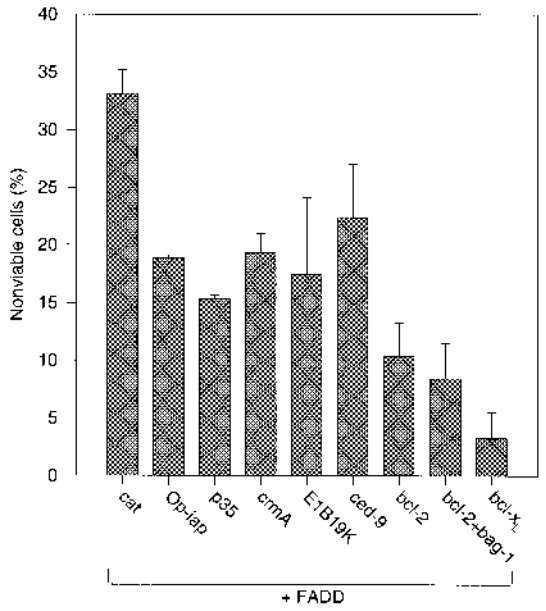

FIG. 7. Protection against FADD-induced cell death in SF-21 cells by antiapoptotic genes. The cells were cotransfected with FADD and either *cat*, Op-*iap*, *p35*, *crmA*, E1B19K, *bcl-2*, *bcl-2* and *bag-1*, or *bcl-x$_L$*. Cell viability was determined by trypan blue exclusion 24 h after the heat shock. The results shown are relative to the viability of cells transfected with *cat* alone and represent at least three independent experiments for each cotransfected combination. Standard deviations are indicated by the error bars.

in Reaper activity. The mutational results, however, do not exclude the possibility that Reaper acts by an oligomerization mechanism similar in nature to that described for the death domain proteins. The data do suggest that Reaper represents a novel type of apoptotic initiator and that it may be worthwhile to consider the existence of homologous genes in mammalian cells.

We also determined whether truncated forms of Reaper could induce apoptosis in SF-21 cells. Neither the C-terminal nor the N-terminal half of Reaper induced apoptosis. Since the N-terminal half lacked epitopes to the antibody we used and expression from the C-terminal half was undetectable, these halves may be inactive, unstable, or both.

Comparison of the nature of apoptotic response induced by *rpr* or FADD in SF-21 cells revealed several distinct features. The extent of cell death and DNA fragmentation induced by *rpr* or FADD was similar, but cytopathic effects and DNA fragmentation induced by FADD expression were observed 24 and 48 h after heat shock induction, respectively, whereas *rpr* induced both of these characteristic apoptotic events by 10 h after heat shock induction (Fig. 2, 6, and 7). Op-*iap* and *p35* efficiently blocked *rpr*-induced cell death and DNA fragmentation, as well as FADD-induced DNA fragmentation. However, FADD-induced cytopathic effects, observed at 24 h after heat shock induction, were only partially inhibited by these two potent baculovirus antiapoptotic genes. Furthermore, unlike *rpr*-induced apoptosis, *bcl-2* and *bcl-x$_L$* inhibited FADD-induced apoptosis. It is possible that FADD induces a type of cytopathic effect which can be blocked efficiently by *bcl-2* and *bcl-x$_L$* but not by Op-*iap* or *p35*. This result suggests the presence of an alternative cell death pathway in SF-21 cells, which eventually converges with the apoptotic pathway. Only one previous report has described an effect of *bcl-2* on insect cell death; Alnemri et al. (1) reported that expression of *bcl-2* can extend the viability of Ac*M*NPV-infected SF-9 cells, a cell line derived from SF-21 cells. However, *bcl-2* was unable to block apoptosis induced by *p35* mutants of Ac*M*NPV (16), suggesting that the type of cell death blocked by *p35* early in infection is different in nature than the cell death that can be delayed by *bcl-2* very late in infection. In a similar way, *bcl-2* or *bcl-x$_L$* may be delaying FADD-induced cell death and preventing the FADD-induced cell death pathway from converging with the apoptotic pathway. The difference in the rate of induction of cell death by *rpr* and FADD and differences in the ability of antiapoptotic genes to block *rpr*- and FADD-induced cell death suggest that apoptosis initiated by these two genes proceeds through distinct pathways. However, the rates of induction of apoptosis by these two genes differ substantially, and we are unable to formally eliminate the possibility that *rpr* induces apoptosis too rapidly to observe inhibition by *bcl-2* or *bcl-x$_L$*.

ACKNOWLEDGMENTS

We are grateful to Jeanne R. McLachlin for critical reading of the manuscript and help in preparing the figures, Alex J. Harvey for construction of pHSDIAP2VI$^+$ and helpful discussions, and Song Yang for continuous encouragement. We thank John M. Abrams (University of Texas) for *rpr* cDNA, Arul M. Chinnaiyan (University of Michigan) for FADD cDNA, John C. Reed (The La Jolla Cancer Research Foundation) for *bag-1* cDNA, Craig B. Thompson (University of Chicago) for *bcl-x* cDNA, H. Robert Horvitz (MIT) for *ced-9* cDNA, Bruce A. Hay (University of California, Berkeley) for D-*iap*2 cDNA, and Winnie W. Wong (BASF Bioresearch Corp.) for *crmA* cDNA. We are also indebted to Gijsbertus J. Pronk (Chiron Corp.) for anti-Reaper antiserum.

This work was supported in part by Public Health Service grant AI38262 from the National Institute of Allergy and Infectious Disease to L.K.M.

REFERENCES

1. **Alnemri, E. S., N. M. Robertson, T. F. Fernandes, C. M. Croce, and G. Litwack.** 1992. Overexpressed full-length human BCL2 extends the survival of baculovirus-infected Sf9 insect cells. Proc. Natl. Acad. Sci. USA **89:**7295–7299.
2. **Beidler, D. R., M. Tewari, P. D. Friesen, G. Poirier, and V. M. Dixit.** 1995. The baculovirus p35 protein inhibits Fas- and tumor necrosis factor-induced apoptosis. J. Biol. Chem. **270:**16526–16528.
3. **Birnbaum, M. J., R. J. Clem, and L. K. Miller.** 1994. An apoptosis-inhibiting gene from a nuclear polyhedrosis virus encoding a polypeptide with Cys/His sequence motifs. J. Virol. **68:**2521–2528.
4. **Boise, L. H., M. Gonzalez-Garcia, C. E. Postema, L. Ding, T. Lindsten, L. A. Turka, X. Mao, G. Nunez, and C. B. Thompson.** 1993. bcl-x, a bcl-2-related gene that functions as a dominant regulator of apoptotic cell death. Cell **74:**597–608.
5. **Boldin, M. P., T. M. Goncharov, Y. V. Goltsev, and D. Wallach.** 1996. Involvement of MACH, a novel MORT1/FADD-interacting protease, in Fas/APO-1- and TNF receptor-induced cell death. Cell **85:**803–815.
6. **Boldin, M. P., I. L. Mett, E. E. Varfolomeev, I. Chumakov, Y. Shemer-Avni, J. H. Camonis, and D. Wallach.** 1995. Self-association of the "death domains" of the p55 tumor necrosis factor (TNF) receptor and Fas/APO1 prompts signaling for TNF and Fas/APO1 effects. J. Biol. Chem. **270:**387–391.
7. **Boldin, M. P., E. E. Varfolomeev, Z. Pancer, I. L. Mett, J. H. Camonis, and D. Wallach.** 1995. A novel protein that interacts with the death domain of Fas/APO1 contains a sequence motif related to the death domain. J. Biol. Chem. **270:**7795–7798.
8. **Borden, K. L., M. N. Boddy, J. Lally, O. R. NJ, S. Martin, K. Howe, E. Solomon, and P. S. Freemont.** 1995. The solution structure of the RING finger domain from the acute promyelocytic leukaemia proto-oncoprotein PML. EMBO J. **14:**1532–1541.
9. **Bump, N. J., M. Hackett, M. Hugunin, S. Seshagiri, K. Brady, P. Chen, C. Ferenz, S. Franklin, T. Ghayur, P. Li, et al.** 1995. Inhibition of ICE family proteases by baculovirus antiapoptotic protein p35. Science **269:**1885–1888.
10. **Chen, P., P. Lee, L. Otto, and J. Abrams.** 1996. Apoptotic activity of REAPER is distinct from signaling by the tumor necrosis factor receptor 1 death domain. J. Biol. Chem. **271:**25735–25737.
11. **Chen, P., W. Nordstrom, B. Gish, and J. M. Abrams.** 1996. grim, a novel cell death gene in Drosophila. Genes Dev. **10:**1773–1782.
12. **Chinnaiyan, A. M., C. G. Tepper, M. F. Seldin, K. O'Rourke, F. C. Kischkel, S. Hellbardt, P. H. Krammer, M. E. Peter, and V. M. Dixit.** 1996. FADD/MORT1 is a common mediator of CD95 (Fas/APO-1) and tumor necrosis

factor receptor-induced apoptosis. J. Biol. Chem. **271:**4961–4965.
13. **Chinnaiyan, A. M., K. Orth, K. O'Rourke, H. Duan, G. G. Poirier, and V. M. Dixit.** 1996. Molecular ordering of the cell death pathway Bcl-2 and Bcl-xL function upstream of the CED-3-like apoptotic proteases. J. Biol. Chem. **271:**4573–4576.
14. **Chinnaiyan, A. M., O. R. K, M. Tewari, and V. M. Dixit.** 1995. FADD, a novel death domain-containing protein, interacts with the death domain of Fas and initiates apoptosis. Cell **81:**505–512.
15. **Chiou, S. K., C. C. Tseng, L. Rao, and E. White.** 1994. Functional complementation of the adenovirus E1B 19-kilodalton protein with Bcl-2 in the inhibition of apoptosis in infected cells. J. Virol. **68:**6553–6566.
16. **Clem, R. J., J. M. Hardwick, and L. K. Miller.** 1996. Anti-apoptotic genes of baculoviruses. Cell Death Differ. **3:**9–16.
17. **Clem, R. J., M. Fechheimer, and L. K. Miller.** 1991. Prevention of apoptosis by a baculovirus gene during infection of insect cells. Science **254:**1388–1390.
18. **Clem, R. J., and L. K. Miller.** 1994. Control of programmed cell death by the baculovirus genes p35 and *iap*. Mol. Cell. Biol. **14:**5212–5222.
19. **Cleveland, J. L., and J. N. Ihle.** 1995. Contenders in FasL/TNF death signaling. Cell **81:**479–482.
20. **Crook, N. E., R. J. Clem, and L. K. Miller.** 1993. An apoptosis-inhibiting baculovirus gene with a zinc finger-like motif. J. Virol. **67:**2168–2174.
21. **Duckett, C. S., V. E. Nava, R. W. Gedrich, R. J. Clem, J. L. Van Dongen, M. C. Gilfillan, H. Shiels, J. M. Hardwick, and C. B. Thompson.** 1996. A conserved family of cellular genes related to the baculovirus iapgene and encoding apoptosis inhibitors. EMBO J. **15:**2685–2694.
22. **Feinstein, E., A. Kimchi, D. Wallach, M. Boldin, and E. Varfolomeev.** 1995. The death domain: a module shared by proteins with diverse cellular functions. Trends Biochem. Sci. **20:**342–344.
23. **Fraser, A., and G. Evan.** 1996. A license to kill. Cell **85:**781–784.
24. **Golstein, P., D. Marguet, and V. Depraetere.** 1995. Homology between reaper and the cell death domains of Fas and TNFR1. Cell **81:**185–186.
25. **Grether, M. E., J. M. Abrams, J. Agapite, K. White, and H. Steller.** 1995. The head involution defective gene of Drosophila melanogaster functions in programmed cell death. Genes Dev. **9:**1694–1708.
26. **Hay, B. A., D. A. Wassarman, and G. M. Rubin.** 1995. Drosophila homologs of baculovirus inhibitor of apoptosis proteins function to block cell death. Cell **83:**1253–1262.
27. **Hay, B. A., T. Wolff, and G. M. Rubin.** 1994. Expression of baculovirus P35 prevents cell death in Drosophila. Development **120:**2121–2129.
28. **Hengartner, M. O., R. E. Ellis, and H. R. Horvitz.** 1992. Caenorhabditis elegans gene ced-9 protects cells from programmed cell death. Nature **356:**494–499.
29. **Hengartner, M. O., and H. R. Horvitz.** 1994. C. elegans cell survival gene ced-9 encodes a functional homolog of the mammalian proto-oncogene bcl-2. Cell **76:**665–676.
30. **Hofmann, K., and J. Tschopp.** 1995. The death domain motif found in Fas (Apo-1) and TNF receptor is present in proteins involved in apoptosis and axonal guidance. FEBS Lett. **371:**321–323.
31. **Hsu, H., H. B. Shu, M. G. Pan, and D. V. Goeddel.** 1996. TRADD-TRAF2 and TRADD-FADD interactions define two distinct TNF receptor 1 signal transduction pathways. Cell **84:**299–308.
32. **Hsu, H., J. Xiong, and D. V. Goeddel.** 1995. The TNF receptor 1-associated protein TRADD signals cell death and NF-kappa B activation. Cell **81:**495–504.
33. **Jaattela, M., M. Benedict, M. Tewari, J. A. Shayman, and V. M. Dixit.** 1995. Bcl-x and Bcl-2 inhibit TNF and Fas-induced apoptosis and activation of phospholipase A2 in breast carcinoma cells. Oncogene **10:**2297–2305.
34. **Kerr, J. F., A. H. Wyllie, and A. R. Currie.** 1972. Apoptosis: a basic biological phenomenon with wide-ranging implications in tissue kinetics. Br. J. Cancer **26:**239–257.
35. **Komiyama, T., C. A. Ray, D. J. Pickup, A. D. Howard, N. A. Thornberry, E. P. Peterson, and G. Salvesen.** 1994. Inhibition of interleukin-1 beta converting enzyme by the cowpox virus serpin CrmA. An example of cross-class inhibition. J. Biol. Chem. **269:**19331–19337.
36. **Lacronique, V., A. Mignon, M. Fabre, B. Viollet, N. Rouquet, T. Molina, A. Porteu, A. Henrion, D. Bouscary, P. Varlet, V. Joulin, and A. Kahn.** 1996. Bcl-2 protects from lethal hepatic apoptosis induced by an anti-Fas antibody in mice. Nat. Med. **2:**80–86.
37. **Liston, P., N. Roy, K. Tamai, C. Lefebvre, S. Baird, G. Cherton-Horvat, R. Farahani, M. McLean, J. E. Ikeda, A. MacKenzie, and R. G. Korneluk.** 1996. Suppression of apoptosis in mammalian cells by NAIP and a related family of IAP genes. Nature **379:**349–353.
38. **Martinou, I., P. A. Fernandez, M. Missotten, E. White, B. Allet, R. Sadoul, and J. C. Martinou.** 1995. Viral proteins E1B19K and p35 protect sympathetic neurons from cell death induced by NGF deprivation. J. Cell Biol. **128:**201–208.
39. **Memon, S. A., M. B. Moreno, D. Petrak, and C. M. Zacharchuk.** 1995. Bcl-2 blocks glucocorticoid- but not Fas- or activation-induced apoptosis in a T cell hybridoma. J. Immunol. **155:**4644–4652.
40. **Miura, M., H. Zhu, R. Rotello, E. A. Hartwieg, and J. Yuan.** 1993. Induction of apoptosis in fibroblasts by IL-1 beta-converting enzyme, a mammalian homolog of the C. elegans cell death gene ced-3. Cell **75:**653–660.
41. **Muzio, M., A. M. Chinnaiyan, F. C. Kischkel, K. O'Rourke, A. Shevchenko, J. Ni, C. Scaffidi, J. D. Bretz, M. Zhang, R. Gentz, M. Mann, P. H. Krammer, M. E. Peter, and V. M. Dixit.** 1996. FLICE, a novel FADD-homologous ICE/CED-3-like protease, is recruited to the CD95 (Fas/APO-1) death-inducing signaling complex. Cell **85:**817–827.
42. **Nagata, S., and P. Golstein.** 1995. The Fas death factor. Science **267:**1449–1456.
43. **O'Reilly, D. R., L. K. Miller, and V. A. Luckow.** 1992. Baculovirus expression vectors: a laboratory manual. W. H. Freeman & Co., New York, N.Y.
44. **Pronk, G. J., K. Ramer, P. Amiri, and L. T. Williams.** 1996. Requirement of an ICE-like protease for induction of apoptosis and ceramide generation by REAPER. Science **271:**808–810.
45. **Quan, L. T., A. Caputo, R. C. Bleackley, D. J. Pickup, and G. S. Salvesen.** 1995. Granzyme B is inhibited by the cowpox virus serpin cytokine response modifier A. J. Biol. Chem. **270:**10377–10379.
46. **Rabizadeh, S., D. J. LaCount, P. D. Friesen, and D. E. Bredesen.** 1993. Expression of the baculovirus p35 gene inhibits mammalian neural cell death. J. Neurochem. **61:**2318–2321.
47. **Ray, C. A., R. A. Black, S. R. Kronheim, T. A. Greenstreet, P. R. Sleath, G. S. Salvesen, and D. J. Pickup.** 1992. Viral inhibition of inflammation: cowpox virus encodes an inhibitor of the interleukin-1 beta converting enzyme. Cell **69:**597–604.
48. **Reed, J. C.** 1994. Bcl-2 and the regulation of programmed cell death. J. Cell Biol. **124:**1–6.
49. **Rothe, M., M. G. Pan, W. J. Henzel, T. M. Ayres, and D. V. Goeddel.** 1995. The TNFR2-TRAF signaling complex contains two novel proteins related to baculoviral inhibitor of apoptosis proteins. Cell **83:**1243–1252.
50. **Schroter, M., B. Lowin, C. Borner, and J. Tschopp.** 1995. Regulation of Fas (Apo-1/CD95)- and perforin-mediated lytic pathways of primary cytotoxic T lymphocytes by the protooncogene bcl-2. Eur. J. Immunol. **25:**3509–3513.
51. **Stanger, B. Z., P. Leder, T. H. Lee, E. Kim, and B. Seed.** 1995. RIP: a novel protein containing a death domain that interacts with Fas/APO-1 (CD95) in yeast and causes cell death. Cell **81:**513–523.
52. **Strasser, A., A. W. Harris, D. C. Huang, P. H. Krammer, and S. Cory.** 1995. Bcl-2 and Fas/APO-1 regulate distinct pathways to lymphocyte apoptosis. EMBO J. **14:**6136–6147.
53. **Sugimoto, A., P. D. Friesen, and J. H. Rothman.** 1994. Baculovirus p35 prevents developmentally programmed cell death and rescues a ced-9 mutant in the nematode Caenorhabditis elegans. EMBO J. **13:**2023–2028.
54. **Takayama, S., T. Sato, S. Krajewski, K. Kochel, S. Irie, J. A. Millan, and J. C. Reed.** 1995. Cloning and functional analysis of BAG-1: a novel Bcl-2-binding protein with anti-cell death activity. Cell **80:**279–284.
55. **Tartaglia, L. A., T. M. Ayres, G. H. Wong, and D. V. Goeddel.** 1993. A novel domain within the 55 kd TNF receptor signals cell death. Cell **74:**845–853.
56. **Tewari, M., and V. M. Dixit.** 1995. Fas- and tumor necrosis factor-induced apoptosis is inhibited by the poxvirus crmA gene product. J. Biol. Chem. **270:**3255–3260.
57. **Tewari, M., L. T. Quan, O. R. K, S. Desnoyers, Z. Zeng, D. R. Beidler, G. G. Poirier, G. S. Salvesen, and V. M. Dixit.** 1995. Yama/CPP32 beta, a mammalian homolog of CED-3, is a CrmA-inhibitable protease that cleaves the death substrate poly(ADP-ribose) polymerase. Cell **81:**801–809.
58. **Uren, A. G., M. Pakusch, C. J. Hawkins, K. L. Puls, and D. L. Vaux.** 1996. Cloning and expression of apoptosis inhibitory protein homologs that function to inhibit apoptosis and/or bind tumor necrosis factor receptor-associated factors. Proc. Natl. Acad. Sci. USA **93:**4974–4978.
59. **Vanhaesebroeck, B., J. C. Reed, D. De Valck, J. Grooten, T. Miyashita, S. Tanaka, R. Beyaert, F. Van Roy, and W. Fiers.** 1993. Effect of bcl-2 proto-oncogene expression on cellular sensitivity to tumor necrosis factor-mediated cytotoxicity. Oncogene **8:**1075–1081.
60. **Vaux, D. L., I. L. Weissman, and S. K. Kim.** 1992. Prevention of programmed cell death in Caenorhabditis elegans by human bcl-2. Science **258:**1955–1957.
61. **Watanabe-Fukunaga, R., C. I. Brannan, N. G. Copeland, N. A. Jenkins, and S. Nagata.** 1992. Lymphoproliferation disorder in mice explained by defects in Fas antigen that mediates apoptosis. Nature **356:**314–317.
62. **White, E., P. Sabbatini, M. Debbas, W. S. Wold, D. I. Kusher, and L. R. Gooding.** 1992. The 19-kilodalton adenovirus E1B transforming protein inhibits programmed cell death and prevents cytolysis by tumor necrosis factor alpha. Mol. Cell. Biol. **12:**2570–2580.
63. **White, K., E. Tahaoglu, and H. Steller.** 1996. Cell killing by the Drosophila gene reaper. Science **271:**805–807.
64. **White, K., M. E. Grether, J. M. Abrams, L. Young, K. Farrell, and H. Steller.** 1994. Genetic control of programmed cell death in Drosophila. Science **264:**677–683.
65. **Wyllie, A. H., J. F. Kerr, and A. R. Currie.** 1980. Cell death: the significance of apoptosis. Int. Rev. Cytol. **68:**251–306.
66. **Xue, D., and H. R. Horvitz.** 1995. Inhibition of the Caenorhabditis elegans cell-death protease CED-3 by a CED-3 cleavage site in baculovirus p35 protein. Nature **377:**248–251.
67. **Yuan, J., S. Shaham, S. Ledoux, H. M. Ellis, and H. R. Horvitz.** 1993. The C. elegans cell death gene ced-3 encodes a protein similar to mammalian interleukin-1 beta-converting enzyme. Cell **75:**641–652.